SAND 90-1721C

Tunnel Damage Resulting from Seismic Loading[1]

J. S. Phillips
Ground Motion Seismic Division

B. A. Luke
Geomechanics Analysis and Testing Division

Sandia National Laboratories
Albuquerque, NM 87185

SYNOPSIS: Correlation of ground motion to observed tunnel damage has largely been based on estimates of ground motion rather than observations and measurements. In an effort to provide a data set that included both measured ground motions and documented tunnel response, an experiment was designed and fielded 0.5 km from a recent underground nuclear explosion (UNE) which had a bodywave magnitude, m_b, and a Richter local magnitude, M_L, of 5.0 (USGS, 1988).

The data obtained in this experiment are summarized in the paper. The discussion centers on the applicability of the results of this experiment to the design of underground facilities for a proposed high-level nuclear waste repository at Yucca Mountain, Nevada.

INTRODUCTION

Damage to underground openings as a result of ground motions, generated by both earthquake and explosive sources, is of interest in many applications and has received considerable study (e.g., Dowding and Rozen, 1978, McClure, 1982; Owen and Scholl, 1981; Pratt, 1982; LaBreche, 1983; Dowding, et al., 1983; Asmis, 1984; and Dowding, 1985). In general, investigators have found that damage to underground openings from ground shaking is less severe than that sustained by surface structures. In addition, case histories indicate that major damage usually involves movement along faults that intersect the opening. Because there is rarely a ground motion measurement located at the point of damage, most analyses have relied on empirical correlations to infer ground motion. An example of a system that relates estimated maximum surface ground motion to tunnel damage is given by Dowding and Rozen (1978). Three damage levels corresponding to maximum particle velocity at the ground surface are given: "no damage" - velocities less than 0.2 m/s; "minor damage" - fall of stones and formation of new cracks, with maximum velocities between 0.2 and 0.9 m/s; and "damage" - major rock falls, severe cracking and closure, with maximum velocities >0.9 m/s). This correlation can be used to assess the potential damage from maximum particle velocities and provide guidance in design for damage mitigation.

---

1. This work was performed under the auspices of the U.S. Department of Energy, Office of Civilian Radioactive Waste Management, Yucca Mountain Project, under Contract DE-AC04-76DP00789.

The proposed high-level nuclear waste repository at Yucca Mountain, Nevada will have many miles of underground openings. Because of the long-term nature of this project (100 yr operating life and containment of waste for 10,000 yr) it is important to gain a high level of understanding of the dynamic behavior of its underground openings. The site, located on and adjacent to the Nevada Test Site (NTS), is subject to seismic loading from both natural events and underground nuclear explosions. While ground motions from both of these seismic sources are of interest to the Yucca Mountain Project, those resulting from earthquakes are expected to be the larger of the two and, therefore, more significant in design. It would be difficult, however, to collect underground data from earthquakes because of their unpredictable nature. In contrast, UNEs have been conducted on a regular basis at the NTS and present an opportunity to obtain data useful in understanding the seismic behavior of underground openings. To this end, the Tunnel Dynamics Experiment (TDE) was fielded adjacent to a recent UNE in a pre-existing tunnel. The objective of this experiment was to document tunnel damage corresponding to measured and observed ground motions.

TUNNEL DESCRIPTION

Construction details of the tunnel test section are shown in Figure 1. This section was initially driven in 1984 with a tunnel boring machine. The corners were mined at a later date producing a drift whose overall dimensions were 6 m high by 5.8 m wide. Rock bolts, 1.8 m long and 2.2 cm in diameter, were placed in the back on a random pattern during the initial mining. Additional bolts, intended for hardening against blasts, were added at a later date. These hardening bolts are 4.9 m long and 2.9 cm in diameter, nominally spaced on 1.2 m centers. All bolts were fully resin-grouted. The tunnel back was lined to the spring line with 4 to 10 cm-thick fiber-reinforced concrete (fibercrete) sprayed over a 5 X 5 cm woven wire mesh. Below the spring line, on both ribs, the wire mesh was placed over the fibercrete. The tunnel invert was covered with approximately 0.3 m of loose gravel.

The test tunnel was excavated in a non-welded ash-fall tuff. Basic rock properties, determined on cores taken from drill holes in the vicinity of the tunnel, are summarized in Table 1. This tunnel had been previously subjected to UNE-generated ground motions of the same order of magnitude measured in the TDE.

TABLE 1. Relevant Rock Properties for the TDE

Density g/cm^3	Unconfined Compressive Strength - MPa	Young's Modulus GPa
1.97	11.0	10.1

Compressive Wave Velocity m/s	Shear Wave Velocity m/s	Poisson's Ratio
2740	1140	0.40

EXPERIMENT DESCRIPTION

The area of study encompassed a 12 m tunnel section located approximately 0.5 km from the explosion. The experiment consisted of acceleration measurements, permanent displacement measurements, tunnel convergence measurements, borehole observations, documentary photography, and high-speed photography. Motion measurements and the high-speed photography experiment were collected in the center of the section. The convergence measurements and borehole studies were conducted at one end of the section, approximately 6 m away from the accelerometers. Permanent displacement measurements and documentary photographs were made over the entire 12 m section. Details of each aspect of this experiment follow.

Triaxial accelerometers were mounted on the ribs, back, and invert of the tunnel (Figure 2), with a triaxial gage package located 9.1 m below the invert. The surface-mounted gages were placed on aluminum plates such that the gage canister assemblies were flush with the tunnel wall. (The tunnel lining was removed from the gage locations before the accelerometer plates were placed.) The free-field gage was grouted in a drill hole 9.1 m below the tunnel invert. All gages were oriented with respect to the longitudinal tunnel axis. Motion perpendicular to the tunnel axis and outward (from the left rib to the right rib) was considered positive radial motion (note that the angle of incidence of the incoming ground motion to the longitudinal tunnel axis was 82°). Positive transverse motion was toward the tunnel portal and positive vertical motion was upward.

Heads of rock bolts on the ribs (which were at about the same height as the accelerometers mounted on the ribs) and the bolts used to mount the gage plates to the tunnel surfaces were used as permanent displacement markers. Pre- and post-test locations of these bolts were documented by third-order surveys. The primary objective of these surveys was to measure large permanent displacements, should they occur. Accuracies of these measurements were within ±1 cm for an individual survey, and ±3 cm from the pre-test to the post-test surveys.

The configuration of tunnel convergence measurement points is shown in Figure 3. Six holes about 3.8 cm in diameter and 48 cm deep were drilled for installation of the tape extensometer anchors: one each in the back and the invert, and two in each rib. The anchors in the invert and back were placed approximately 1 m off-center to avoid interference with the ventilation duct. The anchors, consisting of short lengths of rebar fitted on the ends with eyebolts, were grouted to the rock along nominal 15 cm lengths using resin cartridges. (The hole depths had been overdrilled to permit inspection of the condition of the rock surrounding the anchors.) Convergence measurements were made from the invert to the back (stations 1-2 on Figure 3), left rib to right rib at two elevations (3-4 and 5-6), and invert to left and right ribs (1-3 and 1-4). Back-to-rib measurements were obstructed by tunnel fixtures.

Horizontal boreholes 10 cm in diameter and 9 m deep were drilled into each rib in the same plane as the convergence measurements (Figure 3). These holes were inspected using a borehole video system before and after the explosion in an attempt to assess the extent of changes to the rock mass surrounding the tunnel that might have occurred as a result of the loading.

Optical data obtained in the TDE consisted of high-speed motion photography and documentary still photography. Two redundant high-speed cameras were installed to photograph the immediate vicinity of the accelerometer mounted on the left rib. Still photographs, covering the entire tunnel section, were taken before and after the explosion for the purpose of comparison.

EXPERIMENTAL RESULTS

The bodywave magnitude (m_b) and Richter local magnitude (M_L) of the explosion was 5.0 (USGS, 1988). Maximum free-field ground motions are summarized in Table 2. All maximum amplitudes were generated by the initial compressive wave. The frequencies listed in the table were taken from the power density spectrum calculated for the final filtered time histories and represent the frequency at which the maximum power occurred in the spectrum. The free-field acceleration, velocity, and displacement time histories for the three components of ground motion (Figures 4 through 6) show that even though the maximum acceleration and velocity amplitudes occur in the initial cycle of motion, oscillations continue for approximately 5 s.

TABLE 2. Maximum Free-field Ground Motions

Component	Freq. of Max. Power Hz	Acc. g	Vel. m/s	Disp. cm
Radial	27	27.6	2.3	13.0
Vertical	50	8.8	0.6	-9.7
Transverse	20	4.3	-0.5	-8.5

Ratios of the maximum amplitudes measured on the tunnel walls to the maximum free-field values are presented in Table 3. In most cases, the free-field and tunnel motions were about the same, with notable exceptions of vertical acceleration and velocity on the invert and transverse accelerations on the left rib and invert. Comparisons of velocity time histories of the tunnel surfaces with the free-field motions (Figures 7 through 9) show that tunnel wall motions are similar to free-field motions in terms of both frequency and amplitude. The primary differences between the tunnel surface and free-field motions occur in the initial 0.5 s of motion and are related to the interaction of the incident stress wave with the free surfaces defined by the tunnel walls.

TABLE 3. Ratio of Tunnel Surface Motion to Free-field Motion

Location	Component	Acc.	Vel.	Disp.
Back	Vertical	---*	1.5	0.9
	Radial	---*	0.8	1.3
	Transverse	---*	0.6	0.6
Left Rib	Vertical	2.1	1.3	0.8
	Radial	1.3	1.4	1.1
	Transverse	6.4	1.4	1.4
Right Rib	Vertical	0.8	1.0	0.8
	Radial	0.7	0.8	1.0
	Transverse	0.8	1.0	0.7
Invert	Vertical	3.5	5.2	1.1
	Radial	1.2	0.8	1.0
	Transverse	5.2	1.2	0.4

* Maximum accelerations from this station were questionable.

Permanent displacements, as determined from pre- and post-test surveys of all markers, indicate that the tunnel section translated, as a unit, away from the explosion (about 5 cm) and toward the tunnel face (about 3 cm), with essentially no change in elevation (Figure 10). The left rib moved approximately 1 cm farther radially than the right rib, indicating a reduction in the opening width. No relative horizontal displacement in the cross section was observed between the back and the invert. Vertical displacements indicated that the back and ribs experienced essentially no vertical movement. The invert, however, moved upward approximately 4 cm relative to the other markers, resulting in a reduction in the opening height.

Figure 11 summarizes the convergence measurements made in this tunnel. The greatest closure was measured between the invert and the left rib (4.4 cm) and between the invert and the back (3.8 cm). Both cross-drift measurements showed moderate closure, and the measurement between the invert and the right rib showed slight divergence.

Attribution of directional movement to different parts of the cross section is complicated by the lack of roof-to-rib measurements. In general, the trends observed in these data agree with those observed in the permanent displacement data.

Comparison between the pre- and post-shot borehole inspections (Figures 12 and 13) show marked differences in near-surface conditions. In the left rib borehole, aperatures of preexisting fractures parallel to the opening increased by as much as 3 cm. In the right rib borehole, a new near-surface fracture, 5 cm wide and parallel to the opening, was found post-shot. Changes beyond the first 0.6 m from the surface were limited to a few new hairline cracks at most. Due to limitations of the downhole camera equipment, it is possible that these tiny features had been present pre-shot but were missed in the earlier survey. For the same reason, several similar features that had been logged in the pre-shot survey were not noted afterwards.

The high-speed cameras recorded approximately 380 ms of data. A radial displacement time history was determined by measuring the position of a prominent feature near the left-rib accelerometer on a frame-by-frame basis. The clarity of the image was insufficient to determine a useful vertical displacement. This horizontal displacement and its derived velocity are compared to the data recorded by the accelerometer on the left rib in Figure 14. There is good agreement between these two measurements. The primary difference occurs in the arrival time. This difference may be the result of flash delay at zero time (a flash lamp was used as the zero time indicator for the film) or difficulty in discerning the small initial movements from the image.

Surface damage observed in the still photography was confined mostly to the back and the left rib. This damage was expressed as spalls and cracks in the fibercrete lining as well as some portion of the underlying rock (as confirmed in the borehole observations).

In general, the various types of data gathered in this experiment provided a consistent picture of the dynamic response of this tunnel section. According to Dowding and Rozen's classification system (1978), the damage observed in this tunnel section is categorized as "minor damage."

IMPLICATIONS FOR YUCCA MOUNTAIN FACILITIES

As stated previously, earthquake-generated ground motions are of more concern in design of the YMP facilities than UNE-generated ground motions. In terms of maximum ground motion amplitudes, the tunnel section of the TDE was subjected to a more severe loading than is expected to occur at Yucca Mountain from an earthquake. A major concern, however, is how or even if the results of this experiment can be used to support design of the Yucca Mountain underground facilities. There are two general concerns. The first concern relates to the similarities and differences of the UNE and earthquake sources and the significance of each in terms of tunnel design. The

second concern relates to the differences in the host rock between the TDE site and the Yucca Mountain site. These concerns are discussed below.

Source Comparisons

The major differences between the two seismic sources are summarized below:

- While observed ground motions from both sources consist of compressional and shear waves, explosions produce compression-dominated wavefronts and earthquakes produce shear-dominated wavefronts.
- Duration of shaking from earthquakes is generally longer than observed for UNEs.
- Frequency content of the motions generated by the two sources can be different, depending upon the magnitude of the event and the source-to-station distances.

In general, major damage will occur when the frequency of the ground motion is the same as the natural frequency of the structure. A useful parameter to assess this situation is the ratio of the wavelength (λ) of the seismic disturbance to the width (D) of the opening. When this ratio is large, ($\lambda/D > 8$; for the TDE $\lambda/D > 20$), two simplifications may be made. First, the dynamic amplification of stresses is negligible so design analyses can follow a pseudo-static approach (Labreche, 1983; Hendron and Fernandez, 1983). For the TDE, this was borne out by the similarity of the particle velocities recorded on the tunnel surfaces and the free-field velocities (Figures 7 through 9 and Table 3).[2] Because the wavefront has a large radius of curvature, relative to the tunnel size, the second simplification of a plane wavefront may be made. This implies that strains can be derived from the ratio of maximum particle velocity to material wavespeed (this assumes an elastic, homogeneous, isotropic material). Both shear waves and compression waves produce these strains on underground openings and therefore, the effects of these wave types can be studied on an equivalent basis (Dowding, 1984). If these two simplifications apply, the effects on engineering design of an earthquake-generated shear-dominated wavefront can be predicted based on the response to an explosion-generated compression-dominated wavefront.

To assess differences in duration of shaking, frequency content, and amplitude between earthquake-generated motions and those obtained in the TDE, a prediction was prepared of ground velocities generated by an earthquake of the same magnitude as the UNE. This required a review of analyses of near-source motions from small ($m_b \leq 5.0$) earthquakes. The most appropriate data set found was a number of analyses of ground motions generated by earthquakes and mine tremors in South Africa. These studies have resulted in a series of papers (Spottiswoode and McGarr, 1975; McGarr, Green, and Spottiswoode, 1981;

---

2. Recall stress (σ) is proportional to particle velocity (v), wavespeed (c), and mass density (ρ): $\sigma = \rho c v$.

McGarr, 1981; McGarr, 1982; and McGarr, 1983) on the subject of modeling near-source ground motions and developing source parameters for small earthquakes. A model that predicts a velocity time history was developed in this work and is used here.

The formulation for this model is summarized below. Parameters used in these equations can be in any self-consistent units, unless specified otherwise. The time history equation (McGarr, 1983) is given by:

$$v(t) = 1.28\ v_p\ \omega^2\ t^2\ (3 - \omega t)\ e^{-\omega t} \quad (1)$$

where: v_p is the peak velocity,
t is the time,
ω is $2.34\ \beta/r$,
β is the rock shear wave speed, and
r is the scale of the failure.[3]

$$r_i = 0.1\ (7\ M_o\ /\ 16\ \Delta\tau)^{1/3} \quad (2)$$

where: $\Delta\tau$ is the average stress drop at the failure, and
M_o is the seismic moment.

M_o, in dyne-cm, is determined from:

$$M_o = 17.7 + 1.2\ M_L \quad (3)$$

where: M_L is Richter local magnitude.

Peak velocity is calculated from (McGarr, 1983):

$$v_p = \log^{-1}\ (\ 3.95 + 0.57\ M_L)\ /\ R \quad (4)$$

where: v_p is peak velocity in cm/s, and
R is the hypocentral distance in cm.

The following values were used as input into the model:

- Hypocentral distance, R, was 0.5 km.
- The stress drop was estimated to be 5.0×10^5 dynes. This was based on data from earthquakes and mine tremors with a magnitude range of $1.0 < M_L < 6.4$ and hypocentral distance range of $0.050 < R \leq 1.6$ km which indicate a stress drop range of $10^4 < \Delta\tau < 10^6$ dynes (McGarr, Green and Spottiswoode, 1981).
- β and ρ were taken from Table 1.

---

3. This model assumes a circular fault where r is either source radius (r_o) or most heavily loaded asperity radius (r_i). For this case, we are interested in r_i. Based on the conclusions of McGarr (1982) r_i was assumed to be $0.1\ r_o$.

- The arrival time was assumed to be the same as the TDE.[4]

The velocity time history predicted from this model is compared to the free-field radial velocity time history recorded on the TDE in Figure 15. The significant conclusions from this comparison are

- the maximum amplitude calculated from this model (1.3 m/s) is somewhat less than that measured in the TDE (2.3 m/s).
- the total duration of the time history generated by this model and the TDE are about the same.
- the motion calculated from the model is of much lower frequency than those measured in the TDE.

McGarr (1983) states:

> "... this model is strictly appropriate only for a simple event having a single predominant asperity that fails. To model more complex sources, a series of pulses could be generated with a total duration corresponding to the source time..."

A more complex time history could be produced. However, the parameters necessary to make this more complex prediction are not defined well enough to make the prediction meaningful for this effort. Some heuristic arguments as to what effect these complexities would have on the predicted time history follow.

The source duration for $5.5 < m_b < 5.9$ earthquakes has been estimated to range from 1 to 1.5 s (Doser, 1989; Barker and Wallace, 1986; and Dreger and Helmberger, 1990). In addition, Housner (1970) provides an estimate of the duration of strong phase of shaking of a magnitude 5.0 event as 2.0 s. The more complex time history will likely have a greater duration than the simple waveform predicted due to the fact that the "subevents" will occur at different times with different durations. UNEs have shorter source time durations than earthquakes and the duration of shaking will also be somewhat less. It is important to remember, however, that vertical and transverse ground motions observed in the TDE oscillated at a relatively significant level for about 5 s (Figures 5 and 6). From these observations, it is concluded that the duration of the ground motions recorded in the TDE are consistent within a factor of 2 of what would be expected from an earthquake of similar magnitude. The earthquake will have more cycles of significant amplitude velocities than observed in the TDE, however.

To perform the more complex prediction, the implicit assumption in the procedure is that the motions will be generated by failure of a series of smaller asperities rather than a single large asperity (for the same magnitude event). The asperity size enters in the prediction in the calculation of ω. As r_i becomes smaller, ω becomes larger, which in turn decreases the period of oscillation (Equation 1) and increases

---

4. This simplification was made to facilitate comparison between the TDE waveform and the McGarr model. Because McGarr models shear motion and the inital motion from the TDE is compressional, the arrival times of the two will vary somewhat. Shear motion will arrive after the compressional motion.

the frequency. Therefore, the more complex prediction will be composed of higher frequencies and be more similar to the TDE waveform. However, as long as the λ/D ratio remains relatively large, frequency content differences are insignificant (Hendron and Fernandez, 1983).

Based on this discussion, it appears that the TDE provided a ground motion environment similar to a $m_b = 5.0$ earthquake at a distance of 0.5 km.

Host Rock Comparisons

The second major concern was the differences in mechanical properties of the rock at the TDE and at Yucca Mountain. The host rock for the repository facilities is described as a moderately to densely welded, devitrified ash-flow tuff (Ortiz et al., 1985). The properties of this rock are listed in Table 4. Although the intact rock strength is higher at Yucca Mountain than at the TDE, this rock is extremely brittle and thought to be heavily fractured. If the joints are taken into consideration, the effective strength of the rock mass is considerably less, perhaps on the order of 16 MPa (YMPO, 1989). This dramatic difference in strength emphasizes the need to assess the condition of the rock mass as a whole.

TABLE 4. Relevant Rock Properties for the Repository Host Rock at Yucca Mountain (YMPO, 1989)

Density+ g/cm^3	Unconfined Compressive* Strength - MPa	Young's Modulus* GPa
2.32	155	32.7

Compressive Wave Velocity+ m/s	Shear Wave Velocity+ m/s	Poisson's Ratio+
3400	2040	0.22

\+ Dynamic properties taken from Section 2.1.
* Intact properties taken from Section 1.2.

The two rock masses can be compared using the Rock Mass Rating (RMR) of Bieniawski (1988). The RMR is a well-known means to compare the "constructability" of openings in different rock types, derived from a large, diverse data base. Values are assigned for six parameters; strength of intact rock (q_u), drill core quality (RQD), spacing of joints (j_s), condition of joints (j_c), ground water (w), and orientation of joints with respect to the opening (j_o); then combined to yield a number corresponding to a qualitative description ranging from "very poor rock" to "very good rock." The parameter ratings used to calculate the RMR for the TDE host rock and the repository host

rock are listed in Table 5. Despite significant differences in parameter values, the results for the two very different rock types are similar; both fall in the category of "good rock." This implies that the stand-up times of unsupported openings and the extent of artificial supports required to maintain stable openings in these mechanically dissimilar rock masses are comparable.

TABLE 4. Ratings used to Calculate RMR

Rock	qu	RQD	js	jc	w	jo	RMR
TDE	1	20	20	12	4	0	57
REP	12	13	8	25	15	-12	61

One way to assess the significance of the differences in the rock properties between the TDE and Yucca Mountain is to calculate and compare the maximum strains induced by the ground motion. For the purposes of this discussion, only the maximum circumferential strains will be calculated. For a loading perpendicular to the longitudinal axis of the opening, the circumferential strain is four times the ratio of the maximum particle velocity to the compressive wave velocity of the rock (Hendron and Fernandez, 1983). This comparison assumes a circular cross section, neglects the interaction of the liner, and assumes that the loading and the tunnel construction details are the same in the two rock types. In addition, the assumptions discussed earlier, i.e., a planar wavefront in an elastic, isotropic, and homogeneous medium apply. The circumferential strains calculated for these conditions are 0.34% and 0.27% for the TDE rock and Yucca Mountain rock, respectively. This is a reduction in strain of about 20%. Based on this comparison, it is predicted that a similar tunnel in the Yucca Mountain rock subjected to the same ground motions would sustain "minor damage" in the Dowding and Rozen system (1978).

DESIGN BASIS GROUND MOTIONS

The basis for seismic design of underground facilities at Yucca Mountain has not been explicitly defined. Seismic design bases for an exploratory shaft facility (ESF) and general repository facilities are given (YMPO, 1989). Seismic ground motions specified for the ESF are based on a deterministic analysis of a magnitude 6.5 earthquake 16 km distant. The maximum surface ground motion parameters determined for this design basis were 0.3 g and 0.3 m/s for horizontal acceleration and velocity, respectively. The design basis directs that surface control motions shall be applied at all depths until site characteristics are better quantified. Seismic ground motions specified for the general repository facilities are based on a probabilistic approach (URS/Blume, 1986). In this approach, the specific magnitude and distance of the design event are not provided. In general. however, the design basis ground motions are associated with larger magnitude events at greater distances than in the TDE.

The maximum surface horizontal ground acceleration for this design basis is 0.4 g (as compared to 27.6 g measured in the TDE). No velocities are given and no guidance is provided in this approach for predicting subsurface ground motions. Following is an assessment, based on the concepts discussed in this paper, of the applicability of the TDE results to the current seismic design bases as they relate to underground openings at Yucca Mountain.

Based on the rock properties in Table 4, the frequency characteristics of the design basis for the general repository facilities (URS/Blume, 1986) and the assumption that the repository drifts will have spans ranging from 7.6 to 9.4 m, the λ/D ratio for underground facilities at Yucca Mountain is estimated to range from 11 to 13. According to the earlier discussion, the analysis of these drifts may be done under pseudo-static conditions. The maximum circumferential strain induced by the design basis loading, using the maximum particle velocity specified for the ESF and the same assumptions as before, is estimated to be 0.030%. This is an order of magnitude less than the strains calculated from the TDE loading.

Three important points regarding the proposed repository at Yucca Mountain come from this analysis. First, as long as $\lambda/D > 8$, tunnel motions can be analyzed under pseudo-static conditions. Second, underground openings can be designed to withstand severe transient motions. Finally, ground motions specified in the seismic design basis for the proposed repository, as applied to the underground facilities, are much smaller than those measured in the TDE and can be accommodated in the drift design.

CONCLUSIONS

The conclusions of this study are as follows:

- The TDE produced a consistent data set of measured ground motions and tunnel damage. The maximum radial transient free-field ground motions were 27.6 g, 2.3 m/s, and 13.0 cm. The damage observed in this tunnel was "minor" as defined by Dowding and Rozen (1978).
- Results of the TDE are consistent with case histories discussed in the literature; i.e., only minor damage results, if no significant faults intersect the drift.
- The TDE source stimulated a tunnel response similar to what might be expected in the near-field region of a small-to-moderate (m_b = 5.0) earthquake.
- Comparison of the rock properties between Yucca Mountain and the TDE indicates that a similar tunnel at Yucca Mountain, under the same loading conditions, would have also sustained "minor damage" as defined by Dowding and Rozen (1978).
- Comparison of the TDE ground motions with the design basis motions for Yucca Mountain indicate that the design basis motions are relatively small and can be accommodated in the drift design.

ACKNOWLEDGMENT

The authors acknowledge the support of the Defense Nuclear Agency, especially Joe LaComb, in the fielding of this experiment. Experiment planning assistance was provided by Bob Bass, Chittoor "Subra" Subramanian, Bob Kennedy, and Ray Finley. Jimmy Lee and Cliff Lucas were responsible for fielding the experiment and Jerry Long processed the data. Finally, the encouragement and consultation provided by Marianne Walck was appreciated and is also gratefully acknowledged.

REFERENCES

Asmis, H. W., 1984, Response of Underground Openings in Discontinuous Rock, AECL-7797, Whiteshell Nuclear Research Establishment, Pinawa, Manitoba, Canada.

Bieniawski, Z. T., 1988, "The Rock Mass Rating (RMR) System (Geomechanics Classification) in Engineering Practice," pp. 17-31, Rock Classification Systems for Engineering Purposes, Louis Kirkalde, Ed., ASTM STP 984, American Society for Testing and Materials, Philadelphia, PA.

Barker, J. S., and T. C. Wallace, 1986, "A Note on the Teleseismic Body Waves from the 23 November 1984 Round Valley, California, Earthquake," pp. 883-888, Bulletin of the Seismological Society of America, Vol. 76, No. 3.

Doser, D. I., 1989, "Source Parameters of Montana Earthquakes (1925-1964) and Tectonic Deformation in the Northern Intermountain Seismic Belt," pp. 31-50, Bulletin of the Seismological Society of America, Vol. 79, No. 1.

Dowding, C. H., 1984, "Estimating Earthquake Damage from Explosion Testing of Full-Scale Tunnels," pp. 113-117, Advances in Tunneling Technology and Subsurface Use, Vol. 4, No. 3, Pergamon Press Ltd., Great Britian.

Dowding, C. H., 1985, "Earthquake Response of Caverns: Empirical Correlations and Numerical Modeling," pp. 71-83, Rapid Excavation and Tunneling Conference, Proceedings, Vol. 1, Society of Mining Engineers of AIME.

Dowding C. H., and A. Rozen, 1978, "Damage to Rock Tunnels from Earthquake Shaking," Journal of the Geotechnical Engineering Division, Vol. 104, No. GT2, pp. 175-191, American Society of Civil Engineers.

Dowding, C. H., C. Ho, and T. B. Belytschko, 1983, "Earthquake Response of Caverns in Jointed Rock: Effects of Frequency and Jointing," pp.142-156, Seismic Design of Embankments and Caverns, Proceedings of a Symposium Sponsored by the ASCE Geotechnical Engeering Division in Conjunction with the ASCE National Convention, Philadelphia, PA, May 16-20, 1983, T. R. Howard, Ed., American Society of Civil Engineers, New York, NY.

Dreger, D. H. and D. V. Helmberger, 1990, "Source Characteristics of the February 28, 1990 Upland Sequence from Broad-band Modeling," p. 552, Transactions of the American Geophysical Union, Vol. 71, No. 17, American Geophysical Union.

Hendron, A. J., and G. Fernandez, 1983, "Dynamic and Static Design Considerations for Underground Chambers," pp.157-197, Seismic Design of Embankments and Caverns, Proceedings of a Symposium Sponsored by the ASCE Geotechnical Engeering Division in Conjunction with the ASCE National Convention, Philadelphia, PA, May 16-20, 1983, T. R. Howard, Ed., American Society of Civil Engineers, New York, NY.

Housner, G. W., 1970, "Strong Ground Motion," pp. 75-91, Earthquake Engineering, R. L. Wiegel, Ed., Prentice-Hall, Inc., Englewood Cliffs, NJ.

Labreche, D. A., 1983, "Damage Mechanisms in Tunnels Subjected to Explosive Loads," pp.128-141, Seismic Design of Embankments and Caverns, Proceedings of a Symposium Sponsored by the ASCE Geotechnical Engeering Division in Conjunction with the ASCE National Convention, Philadelphia, PA, May 16-20, 1983, T. R. Howard, Ed., American Society of Civil Engineers, New York, NY.

Langkopf, B. S., and P. R. Gnirk, 1986, Rock-Mass Classification of Candidate Repository Units at Yucca Mountain, Nye County, Nevada, SAND82-2034, Sandia National Laboratories, Albuquerque, NM.

McClure, C. R., 1982, "Damage to Underground Structures During Earthquakes," pp. 75-106, Workshop on Seismic Performance of Underground Facilities, Augusta, GA, 11-13 February, 1981, DP-1623, I. W. Marine, Ed., E. I. du Pont de Nemours & Co., Savannah River Laboratory, Aiken, SC.

McGarr, A., 1981, "Analysis of Peak Ground Motion in Terms of a Model of Inhomogeneous Faulting," pp. 3901-3912, Journal of Geophysical Research, American Geophysical Union, Vol. 86. No. B5.

McGarr, A., 1982, "Upper Bounds on Near-Source Peak Ground Motion Based on a Model of Inhomogeneous Faulting," pp. 1825-1841, Bulletin of the Seismological Society of America, Vol. 72, No. 6.

McGarr, A., 1983, "Estimating Ground Motions for Small Nearby Earthquakes," pp. 113-127, Seismic Design of Embankments and Caverns, Proceedings of A Symposium Sponsored by the ASCE Geotechnical Engeering Division in Conjunction with the ASCE National Convention, Philadelphia, PA, May 16-20, 1983, T. R. Howard, Ed., American Society of Civil Engineers, New York, NY.

McGarr, A., R. W. E. Green, and S. M. Spottiswoode, 1981, "Strong Ground Motion of Mine Tremors: Some Implications for Near-Source Ground Motion Parameters," pp. 295-319, Bulletin of the Seismological Society of America, Vol. 71, No. 1.

Ortiz, T. S., R. L. Williams, F. B. Nimick, B. C. Whittet, and D. L. South, 1985, A Three-Dimensional Model of Reference Thermal/Mechanical and Hydrological Stratigraphy at Yucca Mountain, Southern Nevada, SAND84-1076, Sandia National Laboratories, Albuquerque, NM.

Owen, G. N., and R. E. Scholl, 1981, Earthquake Engineering of Large Underground Structures, FHWA/RD-80/195, National Science Foundation and Federal Highway Administration, Washington, DC.

Pratt, H. R., 1982, "Earthquake Damage to Underground Facilities and Earthquake Related Displacement Fields," pp. 43-74, Workshop on Seismic Performance of Underground Facilities, Augusta, GA, 11-13 February, 1981, DP-1623, I. W. Marine, Ed., E. I. du Pont de Nemours & Co., Savannah River Laboratory, Aiken, SC.

Spottiswoode, S. M., and A. McGarr, 1975, "Source Parameters of Tremors in a Deep-Level Gold Mine," pp. 93-112, Bulletin of the Seismological Society of America, Vol. 65, No. 1.

URS/John A. Blume & Associates, 1986, Ground Motion Evaluations at Yucca Mountain, Nevada With Applications to Repository Conceptual Design and Siting, SAND85-7104, Sandia National Laboratories, Albuquerque, NM.

USGS (U. S. Geological Survey), 1988, Preliminary Determination of Epicenters - Monthly Listing, December, National Earthquake Information Center.

YMPO (Yucca Mountain Project Office), 1989, Yucca Mountain Project Reference Information Base, Version 4, YMP/CC-0002, Sections 1.2 and 2.1, U.S. Department of Energy, Nevada Operations Office/Yucca Mountain Project Office.

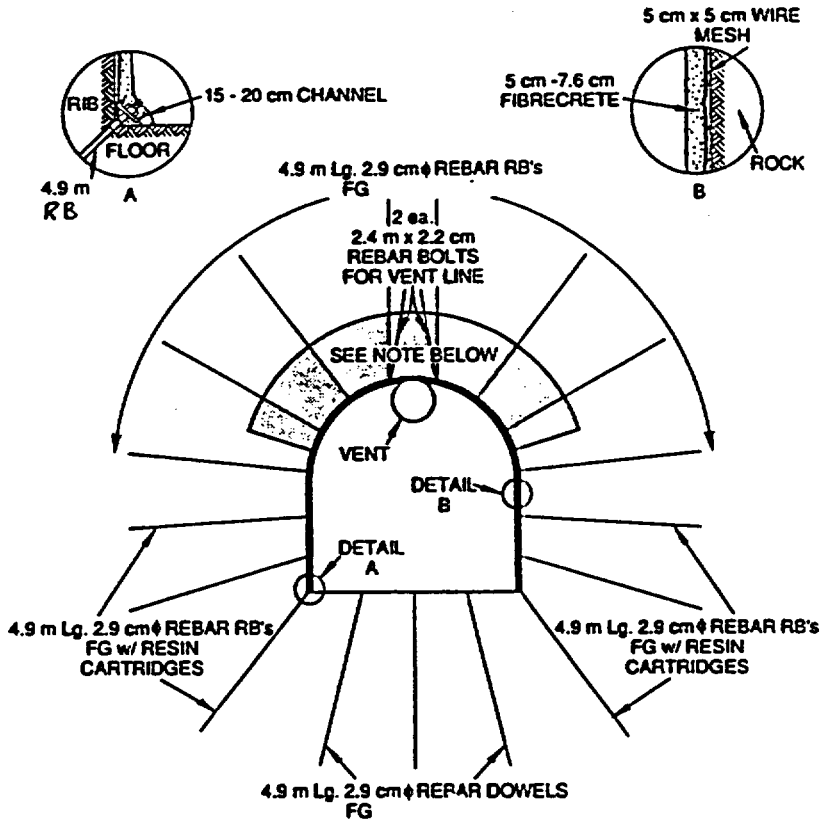

RB's - ROCK BOLTS
FG - FULLY GROUTED
NOTE - AREA WAS BOLTED USING 1.8 m Lg. x 2.2 cm ♦ RB's WHEN MINED w/ TBM ON RANDOM PATTERN. HARDENING BOLTS WERE ADDED AT LATER DATE.

Figure 1. Tunnel Construction Details for the TDE

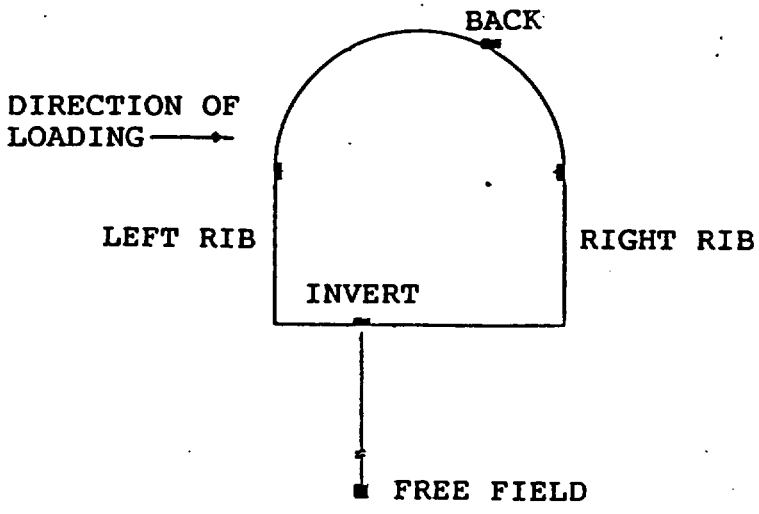

Figure 2. Accelerometer Locations in the TDE

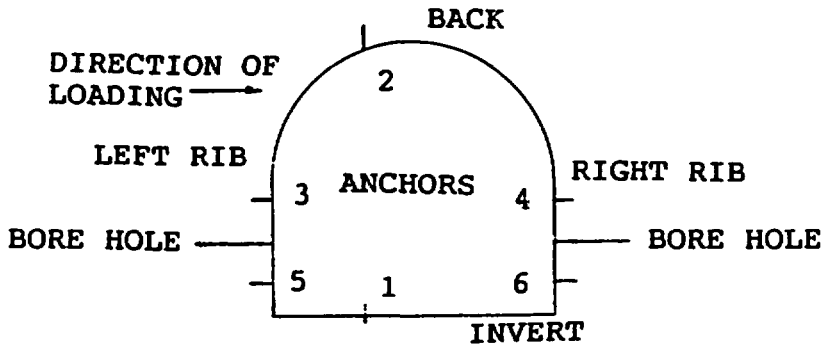

Figure 3. Layout of Tunnel Convergence Measurements and Exploratory Bore Holes

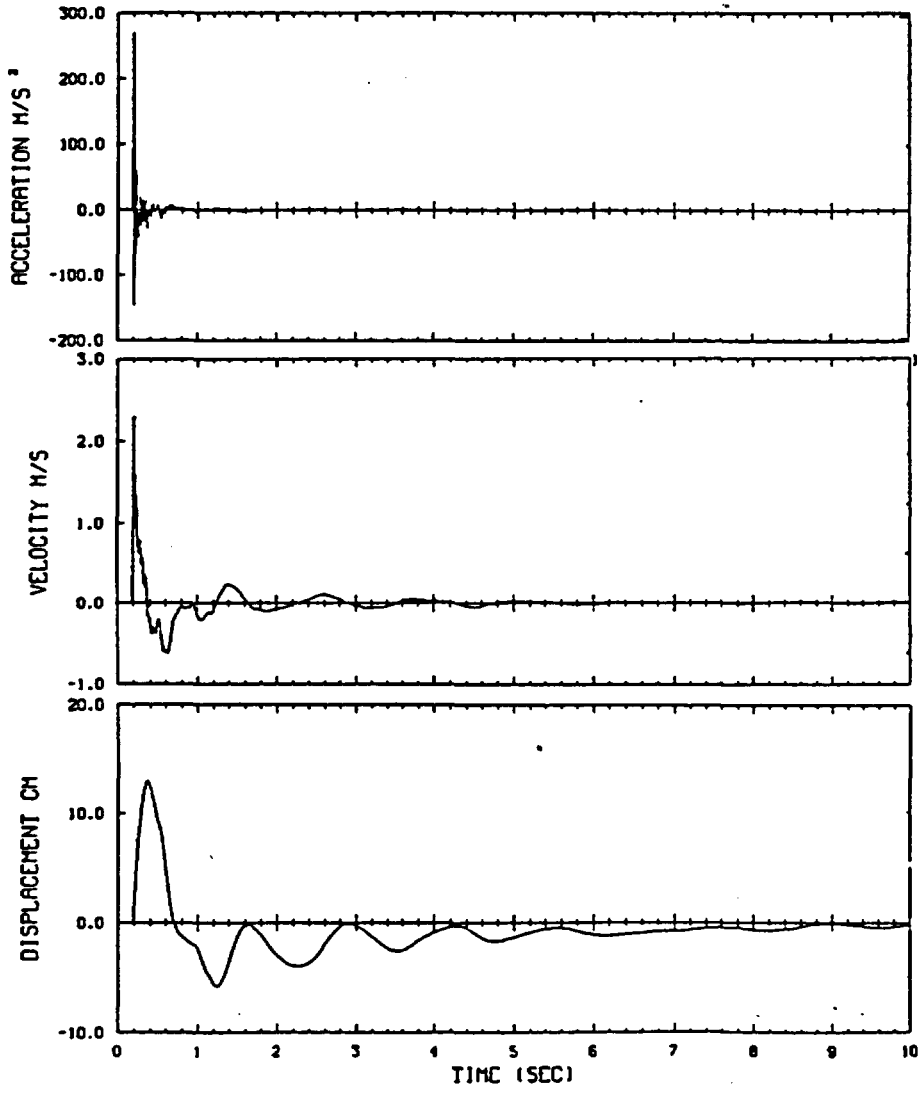

Figure 4. Radial Free-Field Ground Motion Measured in the TDE

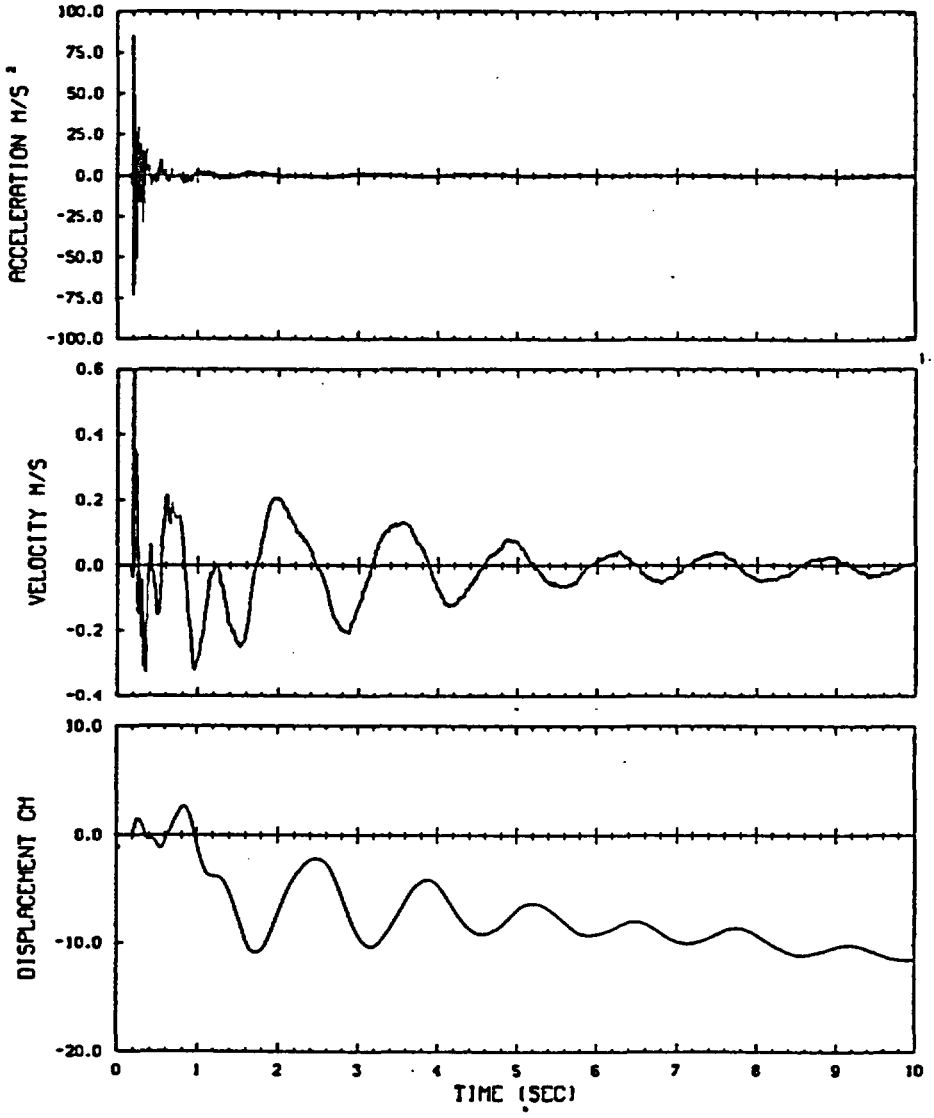

Figure 5. Vertical Free-Field Ground Motion Measured in the TDE

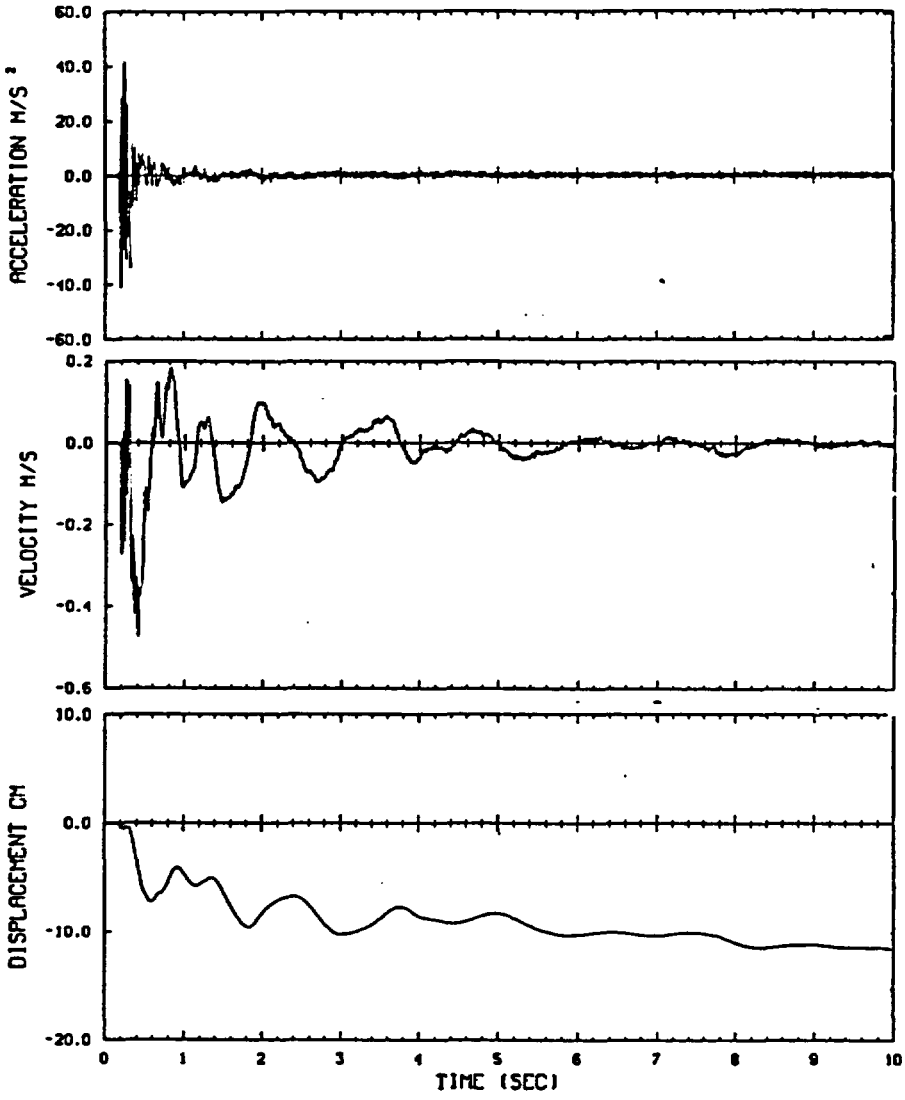

Figure 6. Transverse Free-Field Ground Motion Measured in the TDE

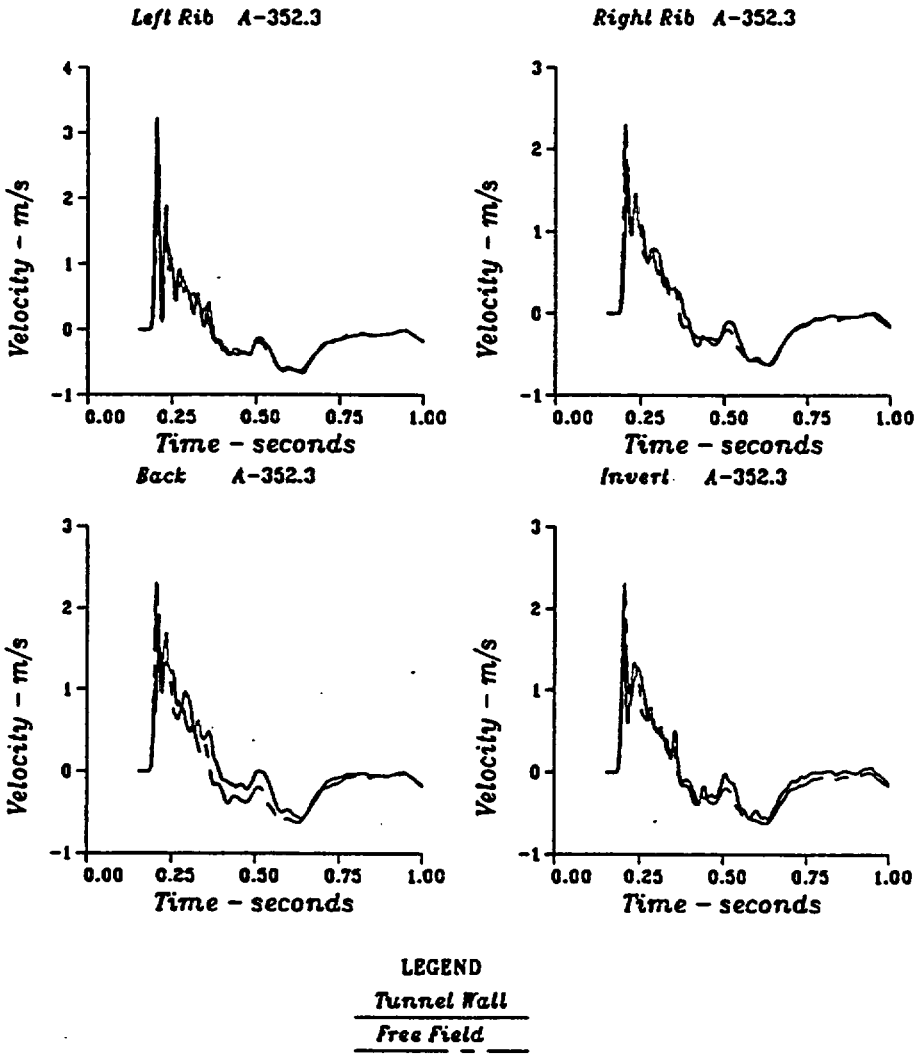

Figure 7. Comparison of Radial Velocities - Free-Field versus Tunnel Wall

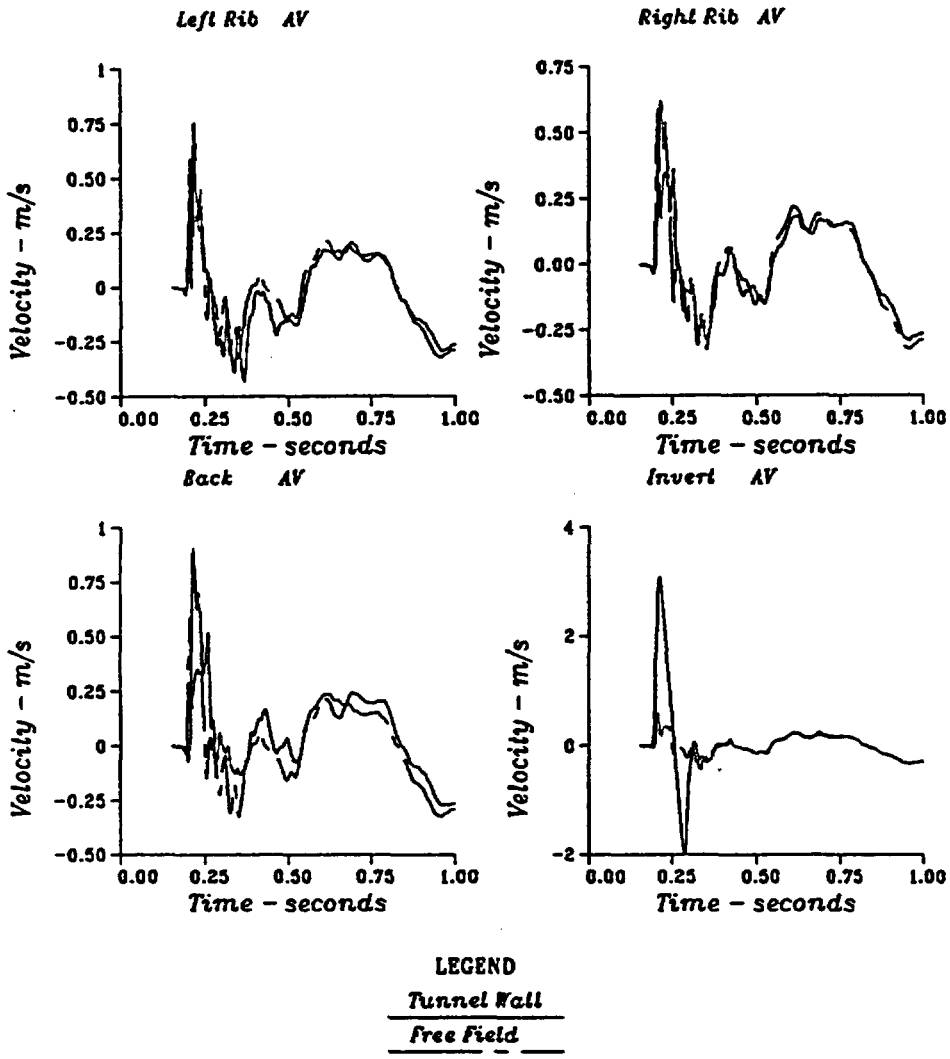

Figure 8. Comparison of Vertical Velocities - Free-Field versus Tunnel Wall

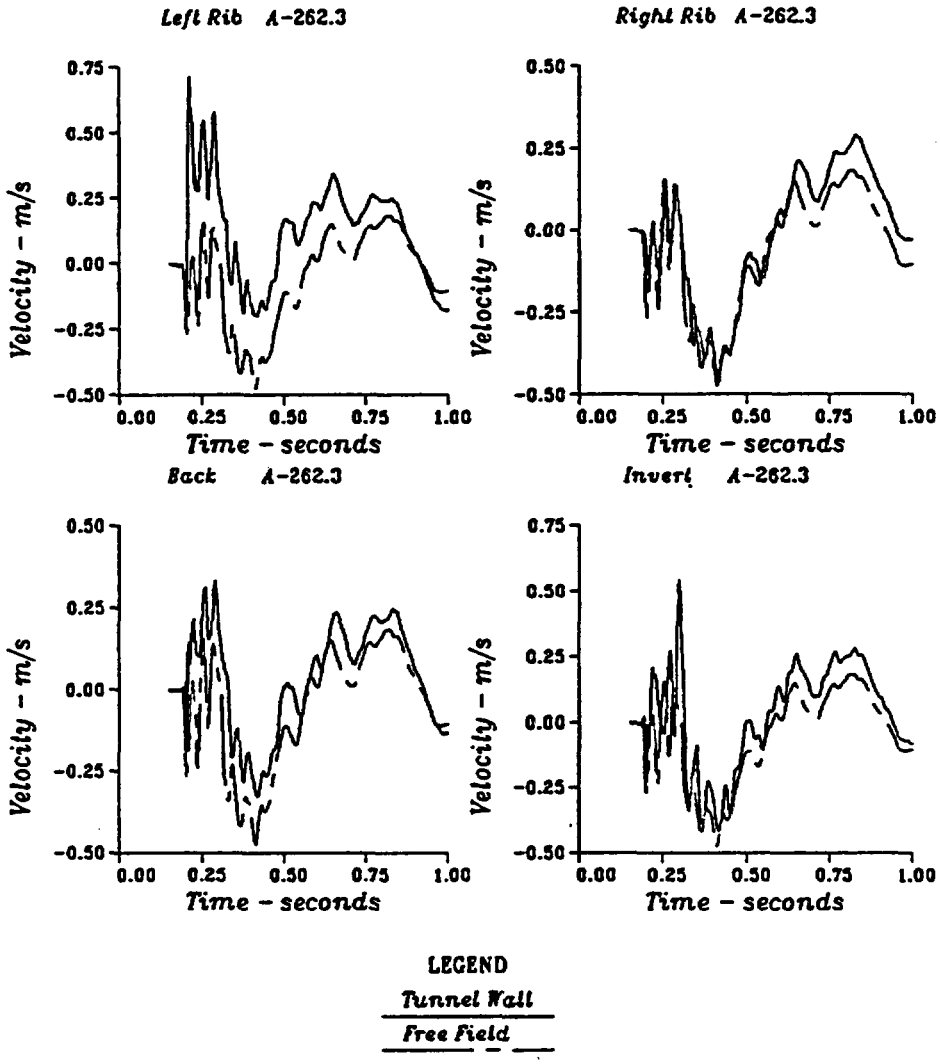

Figure 9. Comparison of Transverse Velocities - Free-Field versus Tunnel Wall

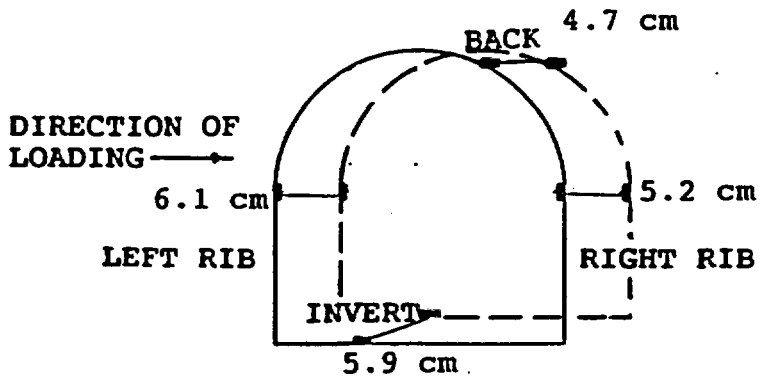

Figure 10. Permanent Displacement of the Tunnel Section

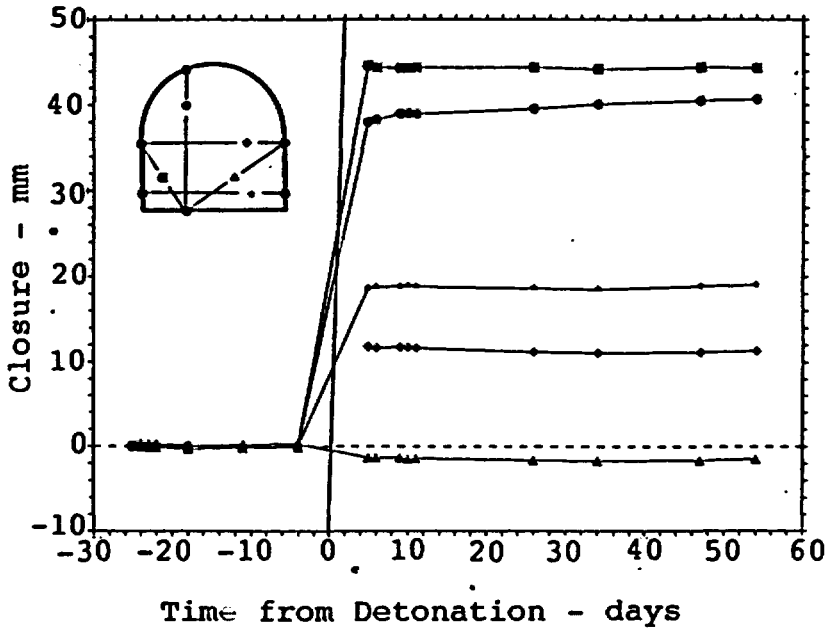

Figure 11. Tunnel Convergence Measurements

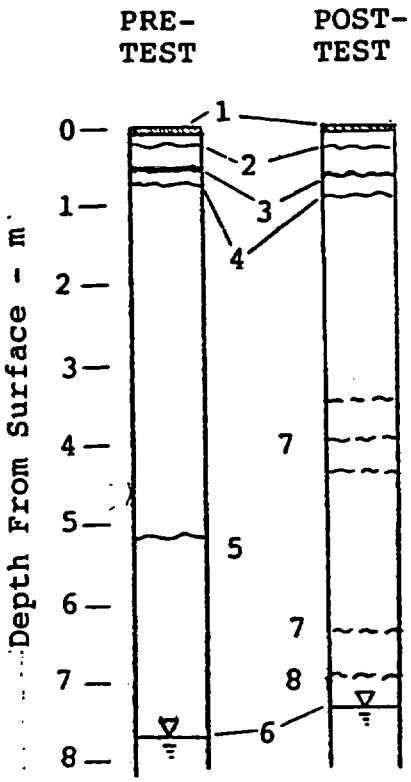

NOTES

1. Fibercrete lining: 10 cm thick pre-test; 5 cm post-test
2. Fracture: 3 cm aperature, pre-test; 4 cm post-test
3. Fracture: 5 cm aperature, pre-test; 8 cm post-test
4. Fracture: 1 cm aperature
5. Hairline crack
6. Standing water
7. Possible hairline cracks
8. Possible fracture: apparent dip ~30°N; aperature ~1 mm

Fractures are vertical fractures and strike parallel to the drift surface. Fractures 2, 3, & 4 were characterized as ragged, loose with no mineralization or infilling. Post-test loose fragments had fallen into borehole.

Figure 12. Comparison of Pre- and Post-test Observations in the Bore Hole on the Left Rib

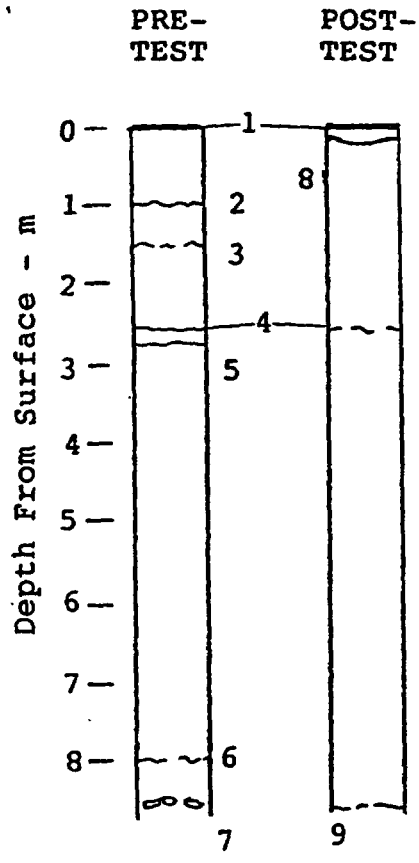

NOTES

1. Fibercrete lining, 8 cm thick
2. Fracture
3. Possible fracture
4. Fracture, dip ~45°N, aperature <0.6 cm, possible mineralization
5. Possible fracture parallel to 4
6. Possible fracture
7. Possible minor spalling
8. Vertical fracture, 5 cm aperature; loose fragments fell into hole
9. Possible fracture

Fractures are vertical and strike parallel to the drift surface, with aperatures <1 mm, except where noted.

Figure 13. Comparison of the Pre- and Post-test Observations in the Bore Hole on the Right Rib

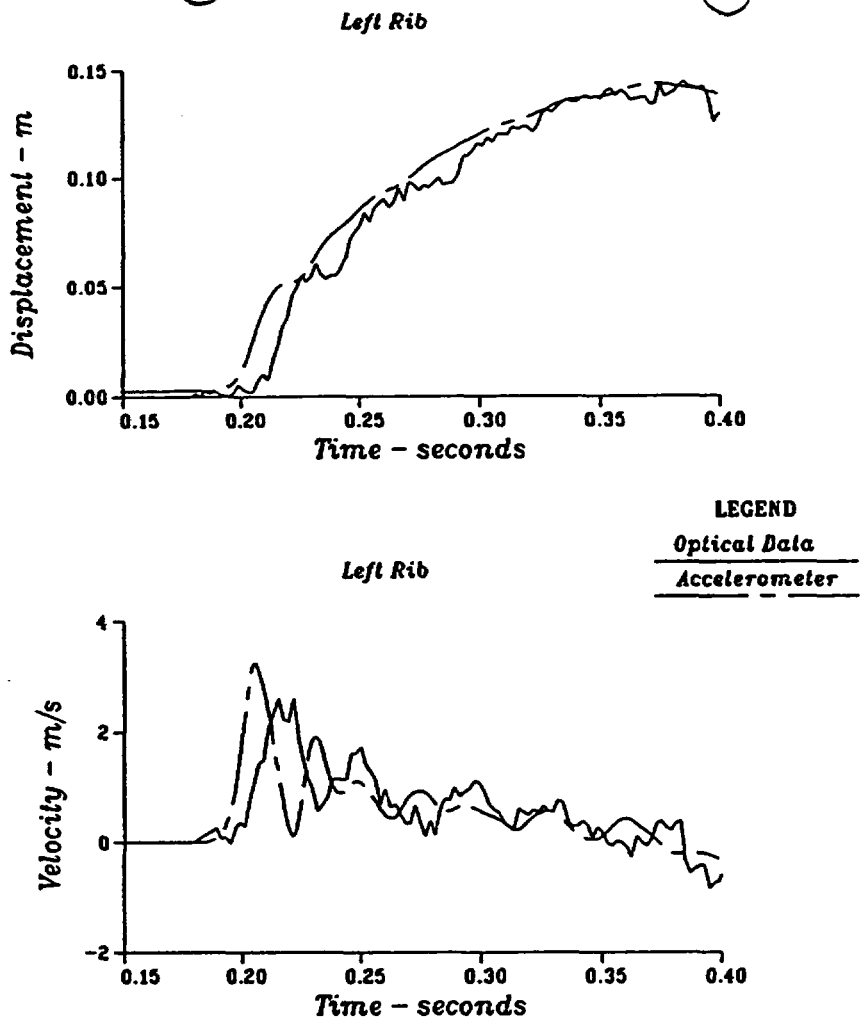

Figure 14. Comparison of the Displacement and Velocity Time Histories Measured by the Accelerometer on the Left Rib and the High-Speed Film.

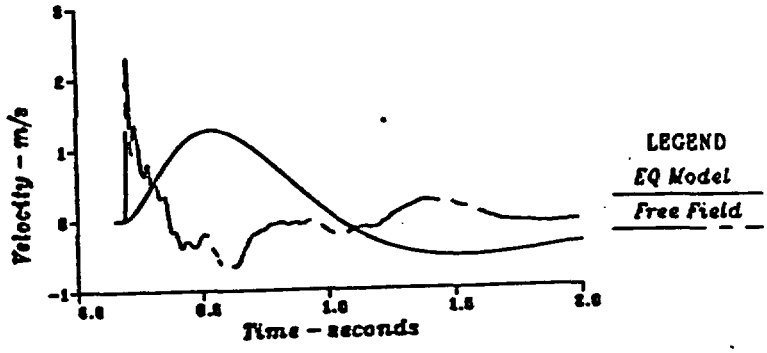

Figure 15. Comparison of the Measured Radial Velocity and Estimates from the McGarr Model

APPENDIX A

This report used data from the Reference Information Base (RIB), as noted in text. This report does not contain any information for the RIB or SEPDB.